Hindawi Publishing Corporation
Journal of Sensors
Volume 2011, Article ID 360173, 5 pages
doi:10.1155/2011/360173

Research Article

Design and Characterization of Nano-Displacement Sensor with High-Frequency Oscillators

Akio Kitagawa

Division of Electrical Engineering and Computer Science, Kanazawa University, Kakuma-machi, Kanazawa 920-1192, Japan

Correspondence should be addressed to Akio Kitagawa, kitagawa@is.t.kanazawa-u.ac.jp

Received 21 April 2011; Accepted 29 June 2011

Academic Editor: Tuan Guo

Copyright © 2011 Akio Kitagawa. This is an open access article distributed under the Creative Commons Attribution License, which permits unrestricted use, distribution, and reproduction in any medium, provided the original work is properly cited.

The circuitry of a capacitive nanometer displacement sensor using the ring oscillator has been analyzed and characterized. We focus on the sensitivity of the sensor to detect the nanometer displacement or strain. The displaced target object must be conductive and the medium around the target object must be an insulator or a vacuum. The sensitivity in the range of $L < 1\,\mu$m is enhanced with decreases in the size of the sensor electrode, and using a higher free-running oscillation frequency can increase sensitivity. The proposed sensor, which converts the displacement of the target object to the oscillation frequency, was fabricated with CMOS 350 nm technology, and the sensitivity was estimated at 8.16 kHz/nm. The results of our study indicated that the presented sensor has enough sensitivity to detect the nanometer displacement of the target object at a distance within 1 μm from the surface of the sensor electrode.

1. Introduction

Proximity sensors and tactile sensors working in the very narrow nominal range can be used to detect microparticles and micromotion of the objects. Furthermore, the integrated proximity sensors have a wide range of applications, such as measurement of the texture, analysis of fingerprints [1], measurement of the tactile or strain distribution [2], and use in touch screens [3]. The proximity sensors and the sensitive displacement sensors in previous studies have been implemented on the basis of various principles of measurement, for example, a capacitive coupling method and some variations with a 30 nm resolution [4, 5], an Eddy current method [6], a millimeter-wave reflection method with a 10 μm resolution of [7], and an integrated Michelson interferometry with a 20 nm resolution [8]. In particular, the capacitive proximity sensors based on an RC oscillation [9] and a delta-sigma modulation [10] offer technical advantages, that is, a higher sensitivity and higher sampling speed because of the higher operating frequency of the electronic circuit as the semiconductor technology is scaled down. The capacitive sensor based on the RC oscillation can be implemented in a very small area, and it is possible to be implanted in the structural element of buildings, machines, and living organisms.

In this paper, we present the circuit analysis of a nanometer displacement sensor, that is, a very high sensitive capacitive proximity sensor, and characterization results of the proposed sensor chip. We focus on the sensitivity of the sensor to detect displacement or strain at the nanometer scale.

2. Circuitry and Sensitivity Analysis

A cross-sectional view of the sensor chip is shown in Figure 1. The top metal is dedicated to the ground electrode and the sensor electrode. The target object forms capacitances C_g and C_s against the sensor electrode and ground electrode. The C_f is a parasitic capacitance between the two electrodes. The capacitances C_g and C_s depend on the distance between each electrode and target object while the capacitance C_f is determined by the geometry of the ground and sensor electrodes. On the assumption that the conductive object has a flat surface, the total capacitance C_A between the electrodes is shown in:

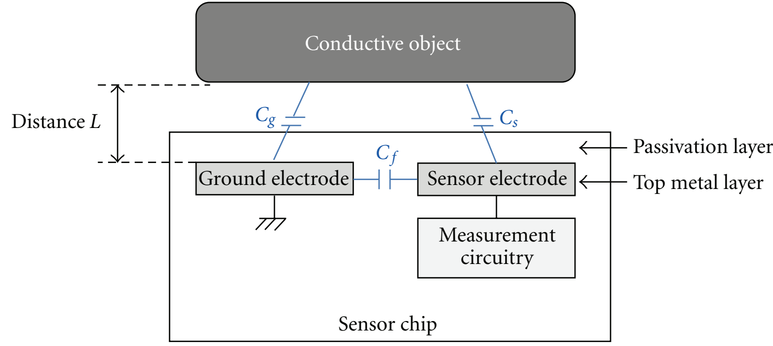

FIGURE 1: Cross-section of sensor chip.

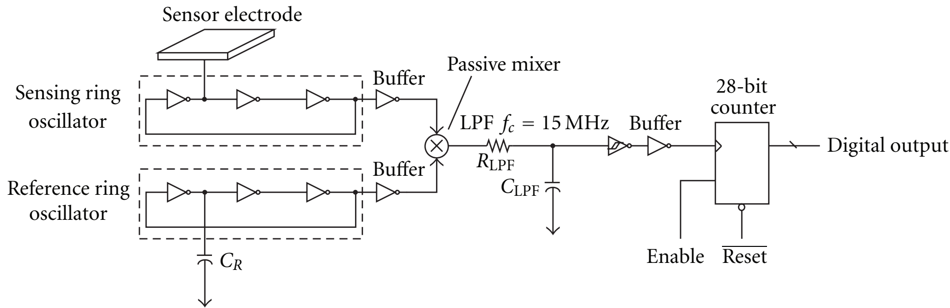

FIGURE 2: Schematic diagram of capacitive sensor with two ring oscillators.

$$C_A(L) = \frac{1}{\left(1/C_g(L)\right) + \left(1/C_s(L)\right)} + C_f = \frac{C_s(L)}{n+1} + C_f \tag{1a}$$
$$\cong \frac{\varepsilon_r \varepsilon_0 S}{(n+1)L} + C_f,$$

$$n = \frac{C_s(L)}{C_g(L)}, \tag{1b}$$

where n is a ratio of C_s and C_g, L is a distance between the bottom of the target object and top surface of the ground or sensor electrodes, S is an area of the sensor electrode, and ε_r and ε_0 are a relative permittivity of the ambient and an electric constant, respectively. If a round-headed tip with the curvature radius R is used as a target object, C_A is replaced by C_{AR} shown in (1c), given that the conductive object is grounded and R is sufficiently smaller than the sensor electrode:

$$C_{AR}(L) = \frac{4\pi \varepsilon_r \varepsilon_0 R}{1 - (R/2(L+R))} + C_f. \tag{1c}$$

A schematic diagram of the circuit detecting a capacitance change of C_A is shown in Figure 2. The sensing ring oscillator is connected to the sensor electrode, and the oscillation frequency f_S changes depending on the value of the capacitance C_A. On the other hand, the reference ring oscillator is connected to the reference capacitance C_R. The oscillation frequency f_R of the reference ring oscillator is fixed by the capacitance C_R. These ring oscillators are adjacently placed each other with a matching layout technique to cancel the difference of electronic characteristics of the transistors. It is difficult to count the oscillation frequency of the ring oscillators because the oscillation frequency of the ring oscillator is very high. The output signals from two oscillators are mixed with each other, and the output frequency of the mixer circuit is converted to $|f_S \pm f_R|$. The RC low-pass filter (LPF) passes the down-converted signal at $|f_S - f_R|$, selectively. The frequency of the down-converted signal is counted by the 28-bit counter. The counting period is controlled by the pulse width of the "Enable" signal, and the bit width of the output value depends on the period of the enable signal. The precision of the frequency measurement is thus inversely proportional to the sampling frequency of the counter output.

The free-running frequency f_{osc} of the 3-stage ring oscillator is determined by the parasitic capacitance C_L in each inverter, transconductance parameter β of MOSFETs (metal-oxide-semiconductor field effect transistor), and power supply voltage V_{DD} according to the following equations [11]:

$$f_{osc} = \frac{1}{6t_{d0}}, \tag{2a}$$

$$t_{d0} = \frac{3.7C_L}{\beta V_{DD}}, \tag{2b}$$

where value t_{d0} is the delay time of the inverters. The extra load capacitance C_A is then added to the sensing ring oscillator, and the frequency f_S of the sensing ring oscillator is estimated as follows:

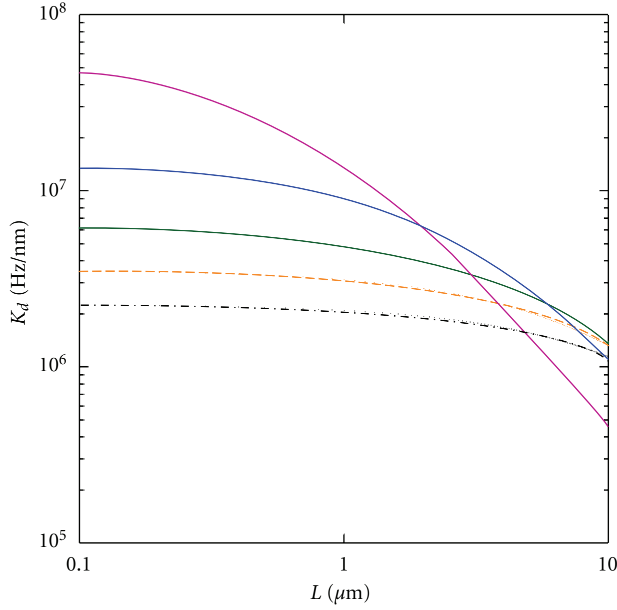

Figure 3: Sensitivity for displacement at L. The curves are calculated assuming CMOS 32 nm technology.

$$f_S = \frac{1}{6t_{d0} + 2\Delta t_d},$$
$$\Delta t_d = \frac{3.7C_A}{\beta V_{DD}} = t_{d0}\frac{C_A}{C_L}. \tag{3}$$

From (1a), (2a), and (3), Equation (4) is derived:

$$f_S = \frac{1}{2t_{d0}(3 + (C_A/C_L))} = \frac{3f_{osc}}{3 + (C_A/C_L)}. \tag{4}$$

The sensitivity of the sensor for the displacement of the target object K_d is found by using (4):

$$K_d = \frac{df_S}{dL} = \frac{df_S}{dC_A}\frac{dC_A}{dL} = \frac{3f_{osc}}{C_L/C_A(L)(3 + (C_A(L)/C_L))^2}\frac{1}{L}. \tag{5}$$

The parameters f_{osc} and C_L depend on the fabrication technology, and C_A is a function of the distance L. The free-running oscillation frequency f_{osc} and the sensitivity of the sensor increase with the advancement of technology node. By using (5) with the assumption that $n = 1$, $\varepsilon_r = 1$ (in vacuum), the sensitivity of the sensor at distance L was estimated by using the typical values of $f_{osc} \sim 55$ GHz and $C_L \sim 0.3$ fF in the CMOS (complementary metal-oxide-semiconductor) 32 nm technology [12]. The L dependence of sensitivity for the size of the sensor electrode is shown in Figure 3.

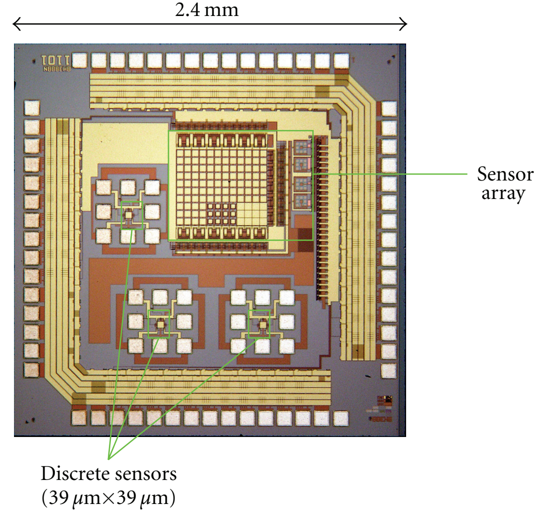

Figure 4: Chip photograph of nano-displacement sensor. Die is 2.4 mm × 2.4 mm, and sensor electrode is 39 μm × 39 μm.

The sensitivity in the range of $L < 1\,\mu$m is enhanced by using a smaller sensor electrode. On the other hand, the sensitivity in the range of $L > 1\,\mu$m decreases with smaller sensor electrode. The displacement of the target in the nanometer scale is detected as a change of the oscillation frequency in the MHz band.

For a round-headed object, the sensitivity for the displacement of the target object is derived based on (1c):

$$K_d = \frac{3f_{osc}}{C_L/C_{AR}(L)(3 + (C_{AR}(L)/C_L))^2}\frac{1}{(L+R)(2L+R)/R}. \tag{6}$$

The L dependence of sensitivity for the round-headed object is similar to the calculation result shown in Figure 3, and the sensitivity is increased with the smaller curvature radius of the object. However, the maximum sensitivity becomes 10 times lower than that for an object which has a flat surface.

3. Results

The sensor circuit presented in Figure 2 was fabricated by using CMOS 350 nm technology. The chip photograph is shown in Figure 4. This chip includes three discrete sensors and an array of 120 sensors. The discrete sensors were used to characterize the shift of the oscillation frequency, and the sensor in the center of the array was used to observe the counter output. With the exception of the active one at the center, all sensor electrodes were connected to the ground by the control signal to switch between the sensor circuit and the ground. The size of the sensor electrode was 39 μm × 39 μm, and the space between the active sensor electrode and the grounded electrode was 10 μm. The size and space of the sensor electrode was not optimized for high sensitivity, but the sensitivity of the sensor with larger electrodes was less affected by the process variation of the chip.

The spectra of the output signal of the sensing ring oscillator are shown in Figure 5. A round-headed tungsten probe

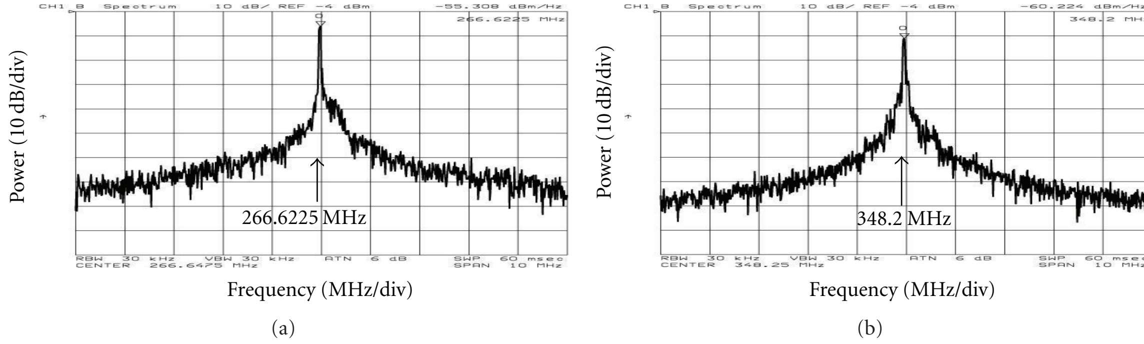

FIGURE 5: Spectra of sensing ring oscillator. (a) Distance from target object was (a) 1 μm and (b) 10 μm. Target object was round-headed tungsten probe with curvature radius of 60 μm.

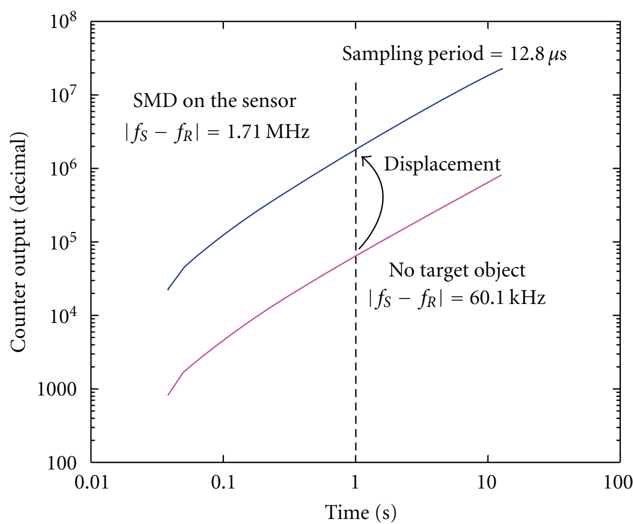

FIGURE 6: Output value of counter versus time. Output period is 12.8 μs. Output value at 1 s implies the frequency of down-converted signal.

with a 60 μm curvature radius was employed as a target object. The capacitance between the tungsten probe and the sensor electrode can be approximated by using the parallel-plates model shown as (1a) because the curvature radius of the target object is larger than the sensor electrode. The oscillation frequencies f_S for $L = 10\,\mu$m and $1\,\mu$m were 266.6225 MHz and 348.2000 MHz, respectively. The sensitivity is estimated at 8.16 kHz/nm. Higher sensitivity is expected in the range of $L < 1\,\mu$m, but the passivation film on the chip obstructed the measurement. The curve of oscillation frequency versus distance will be shown elsewhere after a reattempt to control distance by using an improved chip and an accurate mechanism. The value of the sensitivity is equivalent to that where a 1 nm displacement is measured with precision of 8 bit within 31 ms if there is no phase noise and no fluctuation of the oscillation frequency. The ring oscillator does not have good noise performance. However, the deterioration of the measurement accuracy caused by the influence of the noise can be controlled by the frequency count of the long period. The output value of the counter versus time is shown in Figure 6. The output period is 12.8 μs. These responses are observed with no target object on the sensor chip and in the condition that the surface mount device of the EIA 0603 standard is placed on the sensor surface, respectively. The output value at 1 s implies the frequency of the down-converted signal. The weak nonlinearity of the counter output-time characteristics was observed at 90 ms after the start of measurement. This nonlinearity could be regarded as a result of the temperature drift of the ring oscillator by self-heating.

4. Conclusions

The circuitry of capacitive nanometer displacement sensor using the ring oscillator has been characterized. The sensitivity in the range of $L < 1\,\mu$m is enhanced with decreases in the size of the sensor electrode, and using a higher free-running oscillation frequency increases sensitivity. The proposed sensor was fabricated using CMOS 350 nm technology, and the sensitivity was estimated at 8.16 kHz/nm. It has been shown that the presented sensor has enough sensitivity to detect the nanometer displacement of the target object that is within 1 μm from the surface of the sensor electrode.

Acknowledgments

This work is supported by VLSI Design and Education Center (VDEC), The University of Tokyo in collaboration with Cadence Corporation and Mentor Graphics, Inc. The VLSI chip in this study has been fabricated in the chip fabrication program of VDEC, the University of Tokyo in collaboration with Rohm Corporation and Toppan Printing Corporation. This work was also supported by Grant-in-Aid for Scientific Research (C) (20510116) of Japan Society for the Promotion of Science and Adaptable & Seamless Technology Transfer Program through Target-driven R&D (AS2121327A) of Japan Science and Technology Agency.

References

[1] R. Hashido, A. Suzuki, A. Iwata, T. Okamoto, Y. Satoh, and M. Inoue, "A capacitive fingerprint sensor chip using low-temperature poly-Si TFTs on a glass substrate and a novel and unique sensing method," *IEEE Journal of Solid-State Circuits*, vol. 38, no. 2, pp. 274–280, 2003.

[2] D. Goeger, M. Blankertz, and H. Woern, "A tactile proximity sensor," in *IEEE Sensors*, pp. 589–594, Kona, Hawaii, USA, 2010.

[3] J. Y. Han, "Low-cost multi-touch sensing through frustrated total internal reflection," in *Proceedings of the 18th Annual ACM Symposium on User Interface Software and Technology (UIST '05)*, pp. 115–118, October 2005.

[4] H. Yang, R. Li, Q. Wei, and J. Liu, "The study of high accuracy capacitive displacement sensor used in non-contact precision displacement measurement," in *Proceedings of the 9th International Conference on Electronic Measurement and Instruments (ICEMI '09)*, pp. 164–168, August 2009.

[5] L. K. Baxter, *Capacitive Sensors*, John Wiley & Sons, New York, NY, USA, 1996.

[6] K. Koibuchi, K. Sawa, T. Honma, T. Hayashi, K. Ueda, and H. Sasaki, "Eddy-current type proximity sensor with closed magnetic circuit geometry," *IEEE Transactions on Magnetics*, vol. 43, no. 4, pp. 1749–1752, 2007.

[7] S. Kim and C. Nguyen, "On the development of a multifunction millimeter-wave sensor for displacement sensing and low-velocity measurement," *IEEE Transactions on Microwave Theory and Techniques*, vol. 52, no. 11, pp. 2503–2512, 2004.

[8] D. Hofstetter, H. P. Zappe, and R. Dändliker, "Optical displacement measurement with GaAs/AlGaAs-based monolithically integrated Michelson interferometers," *Journal of Lightwave Technology*, vol. 15, no. 4, pp. 663–670, 1997.

[9] M. Gasulla, X. Li, and G. C. M. Meijer, "The noise performance of a high-speed capacitive-sensor interface based on a relaxation oscillator and a fast counter," *IEEE Transactions on Instrumentation and Measurement*, vol. 54, no. 5, pp. 1934–1940, 2005.

[10] M. Bingesser, T. Loeliger, W. Hinn et al., "Low-noise sigma-delta capacitance-to-digital converter for sub-pF capacitive sensors with integrated dielectric loss measurement," in *Design, Automation and Test in Europe (DATE '08)*, pp. 868–872, March 2008.

[11] D. A. Hodges and H. G. Jackson, *Analysis and Design of Digital Integrated Circuits*, McGraw-Hill, New York, NY, USA, 1983.

[12] The International Technology Roadmap for Semiconductor, *Process Integration, Devices, and Structures*, Sec. Logic Technology Requirements, pp.6–9, 2009, http://www.itrs.net/reports.html.

Journal of
Engineering

The Scientific
World Journal
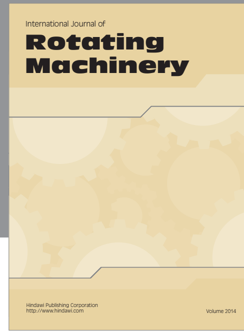
International Journal of
Rotating
Machinery

Journal of
Sensors

International Journal of
Distributed
Sensor Networks
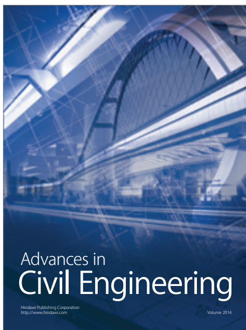
Advances in
Civil Engineering

Hindawi
Submit your manuscripts at
http://www.hindawi.com
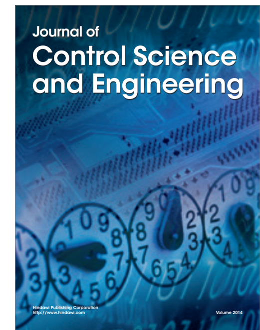
Journal of
Control Science
and Engineering

Journal of
Robotics
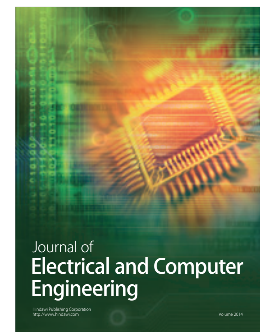
Journal of
Electrical and Computer
Engineering
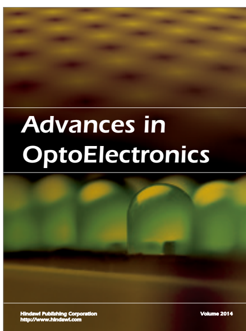
Advances in
OptoElectronics

VLSI Design

International Journal of
Navigation and
Observation
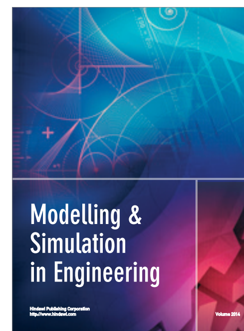
Modelling &
Simulation
in Engineering

International Journal of
Aerospace
Engineering

International Journal of
Chemical Engineering
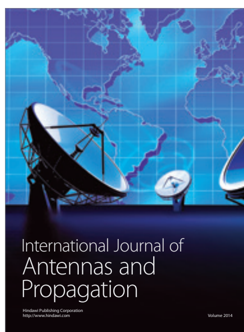
International Journal of
Antennas and
Propagation
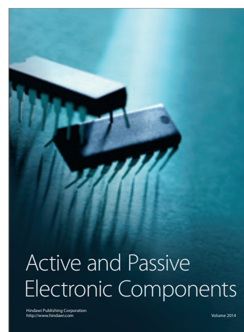
Active and Passive
Electronic Components
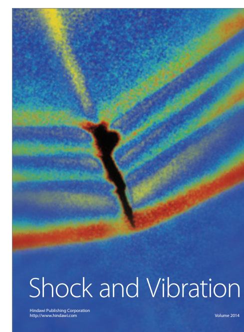
Shock and Vibration
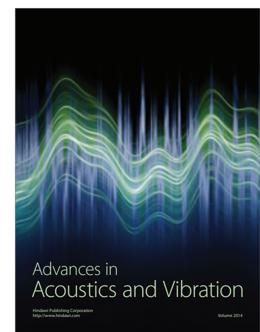
Advances in
Acoustics and Vibration